Modelling the sampling volume for skin blood oxygenation measurements

I. V. Meglinsky[1,2]   **S. J. Matcher[1]**

[1]School of Physics, University of Exeter, Exeter, UK
[2] School of Engineering, Cranfiels Universirty, Cranfield, UK

Abstract—*The absolute quantified measurement of haemoglobin skin blood saturation from collected reflectance spectra of the skin is complicated by the fact that the blood content of tissues can vary both in the spatial distribution and in the amount. These measurements require an understanding of which vascular bed is primarily responsible for the detected signal. Knowing the spatial detector depth sensitivity makes it possible to find the best range of different probe geometries for the measurements of signal from the required zones and group of vessels inside the skin. To facilitate this, a Monte Carlo simulation has been developed to estimate the sampling volume offered by fibre-optic probes with a small source-detector spacing (in the current report $250\,\mu m$, $400\,\mu m$ and $800\,\mu m$). The optical properties of the modelled medium are taken to be the optical properties of the Caucasian type of skin tissue in the visible range of the spectrum. It is shown that, for a small source-detector separation ($800\,\mu m$ and smaller), rough boundaries between layers of different refractive index can play a significant role in skin optics. Wavy layer interfaces produce a deeper and more homogeneous distribution of photons within the skin and tend to suppress the direct channelling of photons from source to detector. The model predicts that a probe spacing of $250\,\mu m$ samples primarily epidermal layers and papillary dermis, whereas spacings of 400–$800\,\mu m$ sample upper blood net dermis and dermis.*

Keywords—*Sampling volume, Light scattering, Human skin, Monte Carlo simulation, Skin blood oxygenation, Multi-layered media*

1 Introduction

SINCE CHANCE introduced the two-wavelength method (CHANCE, 1954), tissue spectraphotometry has been widely applied to different biomedical investigations. Nowadays, optical techniques are most popular for these investigations because light in the visible ($\lambda = 400$–770 nm) and near-infrared (NIR) ($\lambda = 770$–1400 nm) spectral regions makes it possible to monitor changes in microcirculation and haemoglobin oxygen saturation essentially in real time and non-invasively. The results of such measurements within different areas of the skin shed light on a broad range of physiological processes that occur within various skin diseases, such as venous ulcers, skin necrosis, interstitial oedema etc.

As an object of investigation by optical techniques, skin represents a complex heterogeneous medium consisting of distinct layers: epidermis, dermis and subcutaneous fat. These layers contain the chromophores, including DNA, urocanic acid (UCA), amino acids, elastin, collagen, kerratin, NADH, melanin and their precursors and metabolites, whereas the major contribution to light absorption in the visible and NIR spectral regions arises from oxy- and deoxy-haemoglobin (contained in blood), melanin and water (FEATHER *et al.*, 1981; YOUNG, 1997).

Correspondence should be addressed to Dr I.V. Meglinski;
e-mail: i.meglinski@cranfield.ac.uk

Recently, the possibility of using optical reflectance spectroscopy to measure non-invasively skin haemoglobin saturation SO_2 (HANNA *et al.*, 1995) (defined as the ratio of oxygenated to total haemoglobin present in the blood compartment being observed) was introduced. For given carbon dioxide tension and pH, this quantity should bear a fixed relationship to blood pO_2.

However, the absolute quantified measurements of haemoglobin skin blood oxygen saturation from collected reflectance spectra of the skin are complicated by the fact that the blood content of tissues can vary both in the amount and in the spatial distribution. These measurements require an understanding of which vascular bed is primarily responsible for the detected signal. This problem is well known in the related field of laser Doppler flowmetry (JAKOBSSON and NILSSON, 1993; DE MUL *et al.*, 1995).

In the current paper, we report the results of our initial theoretical investigation of the degree of signal localisation to the upper layers of skin (especially the capillary loops). A small source-detector separation in required owing to the shallow spatial location of skin capillary loops (only about $100\,\mu m$ under the skin surface); hence, we cannot reliably apply the diffusion approximation of transport theory for this study (YOO *et al.*, 1990), and only the Monte Carlo technique can provide a realistic model of light propagation in biological tissues. These reasons lead us to choose the Monte Carlo method, which is well-known for its accuracy and simplicity of application to complex multi-layered media (HIRAOKA *et al.*, 1993; JACQUES and WANG, 1995; PRAHL *et al.*, 1989).

2 Computational model of the skin

Following earlier work aimed at computational modelling of the skin (PRAHL *et al.*, 1989; TUCHIN *et al.*, 1994; JACQUES and WANG, 1995), let us consider the skin as a three-dimensional half-infinite medium divided into several layers with varying optical properties (Fig. 1).

The first layer in our model corresponds to a layer of desquamating flattened dead cells, mainly containing keratin, which is 20 μm thick and known as the stratum corneum. The second layer we call 'living epidermis'. It is 80 μm thick and is assumed to contain primarily living cells: a fraction of dehydrated cells, laden cells with keratohyalin granules, columnar cells and also melanin dust, small melanin granules and melanosoms. Given the inhomogeneous distribution of the blood vessels and skin capillaries within the skin, we subdivide the dermis into four different layers, with different blood volumes. These layers are the papillary dermis (150 μm thick), upper blood net dermis (80 μm thick), dermis (1500 μm thick) and deep blood net dermis (170 μm thick). The deepest layer in our model is the subcutaneous fat (6000 μm thick) (see Fig. 1).

Of course, some variability in thickness is expected from region to region of the body and between individuals, and histological evidence suggests this can be of the order of 30–40% (STENN, 1988; ODLAND, 1991; RYAN, 1991). However, we assume that these values for layer thickness are typical of Caucasian adults.

The different structure and blood content of these skin layers affect their optical properties, which is very important for our optical model. The optical properties of the simulated skin layers are μ_a = absorption coefficient, μ_s = scattering coefficient, g = scattering anisotropy factor and n = refractive index. To try to represent the observed histological structure of real skin (see Fig. 1), we model the boundaries of the layers as periodic surfaces (Fig. 2)

$$
\begin{aligned}
B_k(x, y) = Z_k(x_0, y_0) + (A_{kx} \sin(\omega_{ky}x + \phi_{kx}) \\
+ a_{kx} \sin(\omega'_{kx}y + \phi'_{kx}))(A_{ky} \sin(\omega_{ky}y + \phi_{ky}) \\
+ a_{ky} \sin(\omega'_{ky}y + \phi'_{ky}))
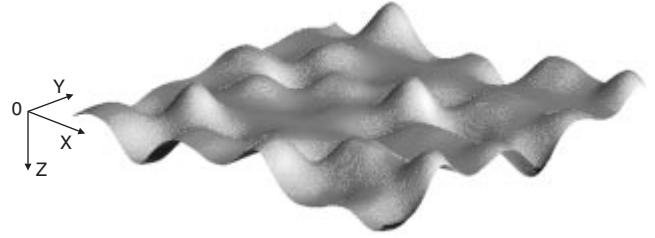\end{aligned}
\tag{1}
$$

Fig. 2 *This surface plot shows the mathematical form used to describe the junction between skin layers in our model, corresponding to a cross-section of a real image of the epidermal boundary*

where $B_k(x, y)$ is the depth of the k layer at (x, y); $Z_k(x_0, y_0)$ is the mean depth of the boundary; k is the layer index; A_{kx}, A_{ky}, a_{kx}, a_{ky} are amplitude coefficients; ω_{kx}, ω_{ky}, ω'_{kx}, ω'_{ky} are scale lengths of the roughness; and ϕ_{kx}, ϕ_{ky}, ϕ'_{kx}, ϕ'_{ky} are arbitrary phase offsets, respectively, in the x- and y-directions. The values of these parameters, presented in Table 1, produce boundaries comparable with the observed structure of real skin (MAIBACH and LOWE, 1987; CORCUFF *et al.*, 1993; HOLBROOK, 1991; ODLAND, 1991; STENN, 1988; RYAN, 1991; SERUP and JEMEC, 1995). Such boundaries are closer to the structure of observed histological sections than plane boundaries (see Fig. 1). This can be important, as the statistics of photon reflections at the boundaries will be affected.

The optical properties of the layers presented in Table 2 are taken from the literature and correspond to a wavelength of 600 nm (SHEUPLEIN, 1964; ANDERSON and PARRISH, 1982; CHEONG *et al.*, 1990; DUCK, 1990; NILSSON and NILSSON, 1998; RAJADHYAKSHA and ZAVISLAN, 1998; TUCHIN, 1998; SCHMITT and KUMAR, 1998; SIMPSON *et al.*, 1998; DOORNBOS *et al.*, 1999).

3 Method

The method for simulating the sampling volume for the different fibre-optic probe geometries is based on the random simulation of a large number of possible trajectories of photons
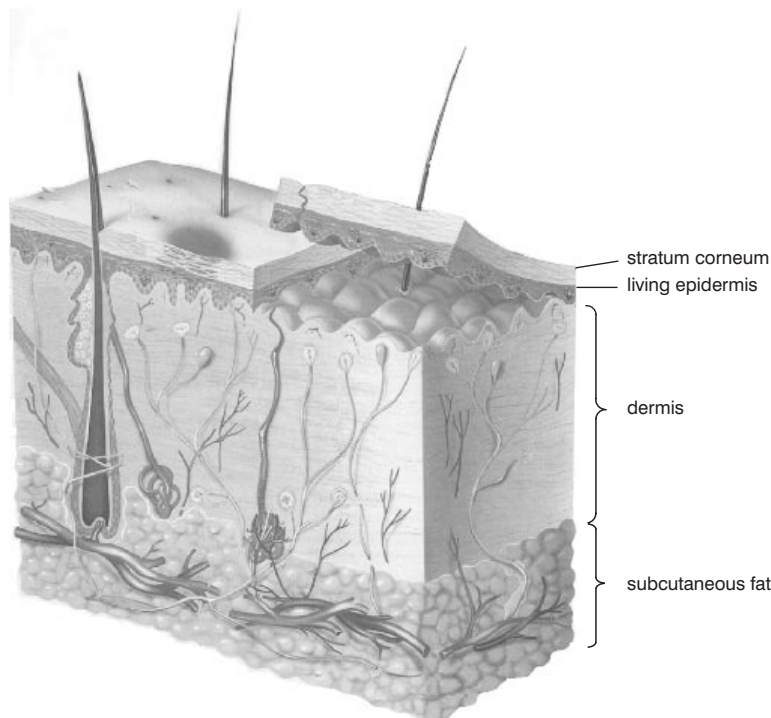

Fig. 1 *Skin structure*

Table 1   Values of parameters defined in eqn 1 and used in our simulation

k	Boundary between layers	A_{kx}, A_{ky}, µm	$(\pi/\omega)_{kx}$, µm	$(\pi/\omega)_{ky}$, µm	$Z_k(x_0, y_0)$, µm
0	air – startum corneum (skin surface)	2	100	150	0
1	startum corneum – living epidermis	2.5	80	80	20
2	living epidermis – papillary dermis	20	50	45	100
3	papillary dermis – upper blood net dermis	2	20	40	200
4	upper blood net dermis – dermis	2	20	50	280
5	dermis – deep blood net dermis	2	20	50	1900
6	deep blood net dermis – subcutaneous fat	5	20	50	2100
7	subcutaneous fat – other tissues	5	25	30	8000

as they travel through the highly scattering medium. The simulation consists of a sequential random walk of photon packets between scattering events from the site of photon injection into the medium to the site where the photon leaves the medium. The random path length that a photon packet moves for step i is given by

$$l_i = -\frac{\ln(\xi_i)}{\mu_s} \qquad (2)$$

where ξ_i is a uniformly distributed random number between 0 and 1. After injection into the medium, a software-generated random number is used to determine the distance propagated before the photon packet encounters the next scattering centre. The scattering event is then simulated by the generation of two random propagation angles φ and θ, which describe the new direction in which the photon packet then travels. The whole process is repeated until the photon packet either exits the tissue or is lost within the medium. The principles of this method have been widely described (CASHWELL and EVERETT, 1959; MEIER *et al.*, 1978; PRAHL *et al.*, 1989; JACQUES and WANG, 1995; WANG *et al.*, 1995).

In our model, we have taken into account the internal reflection of the scattered radiation on the medium boundary by allowing the incident photon packet to split into a reflected and transmitted part (VAN DER ZEE, 1992). The weight of these reflected and transmitted parts of the photon packet are attenuated according to the Fresnel reflection coefficients (BORN and WOLF, 1986)

$$R(\alpha) = \begin{cases} \left(\frac{n_{k+1}-n_k}{n_{k+1}+n_k}\right)^2 & \text{if } \alpha = 0 \\ \frac{1}{2}\left[\frac{\sin^2(\alpha-\alpha_t)}{\sin^2(\alpha+\alpha_t)} + \frac{\tan^2(\alpha-\alpha_t)}{\tan^2(\alpha+\alpha_t)}\right] & \text{if } 0 < \alpha < \sin^{-1}\left(\frac{n_{k+1}}{n_k}\right) \\ 1 & \text{if } \sin^{-1}\left(\frac{n_{k+1}}{n_k}\right) < \alpha < 90 \end{cases} \qquad (3)$$

where the symbols are defined in Fig. 3.

Table 2   Optical properties of skin model ($\lambda = 600$ nm, Caucasian skin)

k	Skin layer	μ_s, mm^{-1}	μ_a, mm^{-1}	g	n
1	stratum corneum	100	0.02	0.9	1.53
2	living epidermis	40	0.015	0.85	1.34
3	papillary dermis	30	0.07	0.8	1.4
4	upper blood net dermis	35	0.1	0.9	1.39
5	dermis	20	0.07	0.76	1.4
6	deep blood net dermis	35	0.1	0.95	1.39
7	subcutaneous fat	15	0.03	0.8	1.44

The refractive index of air is $n_0 = 1$

Thus, in the absence of absorption, the probability of collecting a photon on the detector is described as follows:

$$W_0 = W_{in}(1 - R_0(\alpha)) \prod_{p=1}^{B} R_p(\alpha) \qquad (4)$$

where W_{in} is the initial weight of the photon packet, B is the number of times the photon packet undergoes a partial reflection on the medium boundary, $R_p(\alpha)$ is the Fresnel reflection coefficient for the pth photon–boundary interaction, and $R_0(\alpha)$ is the Fresnel reflection coefficient for the initial photon packet–boundary interaction, when the photon packet enters the medium.

To decide whether a photon is reflected or transmitted at internal layer boundaries in the medium ($k \neq 0$), we follow the procedure of JACQUES and WANG (1995), i.e. compare a random number ξ_B uniformly distributed between 0 and 1 to $R(\alpha)$ (3) and allow either reflection or transmission of the photon if ξ_B is smaller or bigger than $R(\alpha)$, respectively.

The simulation of an individual photon packet is stopped if its statistical weight falls below 0.001, or if it moves away from the source by more than 1000 scattering mean free-paths, or if the total number of scattering events exceeds 10 000. The total number of detected photon packets N_{ph} (usually 10^5–10^7) used for each simulation is defined before the simulation (KIENLE *et al.*, 1996). The individual trajectory of each detected photon packet are stored in a data file, requiring a large amount of disk memory (typically several hundred megabytes).
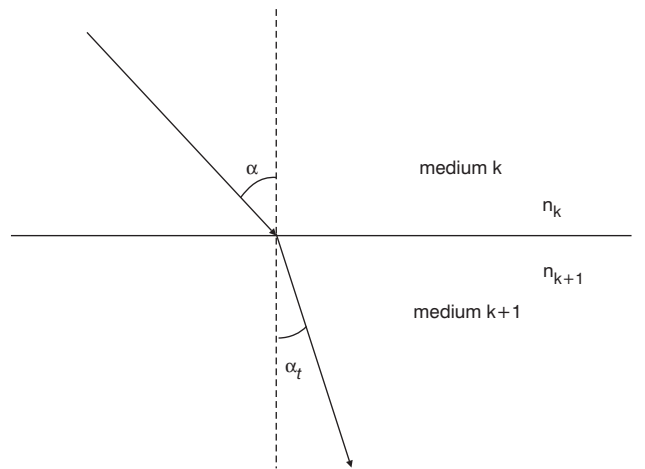

Fig. 3   *The diagram represents the reflected and transmitted parts of the photon packet on the medium boundary. Here, α and α_t are the angles of the photon packet incidence on the layer boundary and transmittance, respectively, k and $k + 1$ show the direction of the photon packet–boundary crossing and indicate the medium layers (0 corresponds to the ambient medium); n is the refractive index*

According to the microscopic Beer–Lambert law, we include absorption of photons within the medium layers by recalculating the statistical weight of each photon packet according to the length of its trajectory within the layer. Thus, the final weight of the photon packet on the detector is described as follows:

$$W_{a,j} = W_0 \cdot \exp\left(-\sum_{i=1}^{M} \mu_a(\boldsymbol{r}_i) l_j(\boldsymbol{r}_i)\right) \quad (5)$$

where M is the number of voxels in the simulated volume, and $\mu_a(\boldsymbol{r}_i)$ and $l_j(\boldsymbol{r}_i)$ are, respectively, the absorption coefficient and the path length traversed by the jth photon packet in voxel i at position $\boldsymbol{r}_i$.

The sampling volume, i.e. spatial distribution of detector depth sensitivity $Q(\boldsymbol{r}_m)$, is defined as the gradient of optical density with respect to absorption coefficient μ_a at each pixel $\boldsymbol{r}_m$ in the medium (HIRAOKA et al., 1993; ARRIDGE, 1995)

$$Q(\boldsymbol{r}_m) = -\frac{\partial}{\partial \mu_a(\boldsymbol{r}_m)} \ln\left(\frac{I}{I_0}\right) = \frac{\sum_{j=1}^{N_{ph}} W_{a,j} l_j(\boldsymbol{r}_m)}{\sum_{j=1}^{N_{ph}} W_{a,j}} = \langle l(\boldsymbol{r}_m) \rangle \quad (6)$$

Here, $I = \sum_{j=1}^{N_{ph}} W_{a,j}$, $W_{a,j}$ is the statistical weight of the jth detected photon (eqn 5); $l_j(\boldsymbol{r}_m)$ is the path length traversed by the jth photon packet in the mth pixel at a position $\boldsymbol{r}_m$; and $\langle l(\boldsymbol{r}_m) \rangle$ is the weighted mean of the path length traversed by each photon through pixel m. In the current simulation, we consider the distribution $Q(\boldsymbol{r}_m)$ as a function of x and z only, where x is the horizontal axis referred to the centre-to-centre line between source and detector, and z is the depth direction; i.e., $Q(x, z)$ represents a two-dimensional cross-section map through the 3D distribution $Q(\boldsymbol{r}_m)$. It can be shown (HIRAOKA et al., 1993; ARRIDGE, 1995; OKADA et al., 1997) that this quantity equals the mean path length travelled by photons within the cell at $\boldsymbol{r}$. Hence, in our simulation, $Q(\boldsymbol{r}_m)$ is calculated directly from the photon history data.

4 Results and discussion

Simulated spatial distributions of detector depth sensitivity in the case of wavy interfaces between the layers are presented in Figs 4a, c and e and are compared with the results of simulations with flat layer boundary interfaces in Figs 4b, d and f. The photon history has been calculated using 10^4 detected photon packets for each model, and the calculation time on a Silicon Graphics RS00 Indy workstation took about 1 h for 10^3 photon packets. The source-detector fibre spacing (800 µm, 400 µm and 250 µm (centre-to-centre)) and diameters (200 µm and 50 µm, respectively) were largely determined by the practicalities of the fibre-optic probe design and manufacture. The sizes of the grid cells used in the simulation were chosen to be 10 µm in the x-, y-, and z-directions.

The spatial distribution of detector depth sensitivity $Q(x, z)$ has units of millimetres, representing the average physical path travelled by photons in the pixel located at (x, z). The asymmetry in the distribution near the source and detector areas seen in Figs 4a–f is due to the different size of the source and detector fibres. It is noteworthy here that, for all values of source–detector spacing (see Figs 4a–f), the detector is most sensitive to the uppermost highly scattering and absorbing layer, the thickness of which is 100 µm or less. In other words, the majority of the incident radiation reaches only the first layer of the skin. This result agrees well with the known properties of skin, where the stratum corneum and epidermis stop the majority of the light incident on the skin surface (SLINEY and WOLBARSHT, 1980; TUCHIN, 1998).

However, skin blood oxygenation measurements require us to sample deeper layers of skin, because the capillary loops are typically located at a depth of about 100–150 µm under the skin surface. Increasing the source–detector spacing to 800 µm increases the sampling volume, so that it reaches the middle of the dermis (Figs 4a and b). The detected signal should be collected now from the top part of the dermis, which includes the capillary loops, small venules and arterioles. Decreasing the source–detector spacing significantly reduces the area over which the detector is sensitive (see Figs 4e and f).

For the distribution of detector depth sensitivity $Q(x, z)$ for the medium with flat layer boundary interfaces (see Figs 3b, d and f) along the boundaries of the first two layers (in depth 0, 20, 100 and 200 µm) we can see small 'channels' between the source and detector areas. The simulations using wavy boundary interfaces between layers tend to suppress these 'channels' (see Figs 4a, c and e) and lead to photon packets being distributed more homogeneously within the medium (see Fig. 4a). Comparing the results of the simulations using wavy interfaces with those using flat interfaces, we can see that the influence of the wavy boundaries is also pronounced in reducing the internal reflection of photon packets on the medium surface. This is evident as a suppression of the channels between source and detector (see Figs 4a and b, c and d).

To compare the results quantitatively, it is better to consider the mean partial optical path length

$$\langle l_k \rangle = \frac{-\partial \ln\left(\frac{I}{I_0}\right)}{\partial \mu_{a,k}} \quad (7)$$

for each layer as a function of the source–detector spacing. Here $\partial \mu_{a,k}$ represents a perturbation to μ_a that occurs uniformly throughout layer k.

An increase in blood content in a layer will tend to reduce the overall path length in that layer; conversely, a decrease in blood content will lengthen the path length in it. However, we believe that the blood content used in our simulation is a reliable estimate for the true blood volume in the skin tissues.

Fig. 5 shows the fraction of total path length in the first five layers of both media with wavy (Fig. 5a) and flat (Fig. 5b) layer boundaries as a function of the source–detector spacing. It can be seen that the fraction of total path length in the first two layers decreases as the source–detector spacing increases up to 800 µm (see Fig. 5), whereas, in other layers, the mean path length increases with increasing source–detector spacing. It is evident that, in the case of wavy boundaries, the photon packets penetrate deeper into the medium (see Fig. 5a).

Thus, alteration of the photon reflection/refraction rules on the layer boundaries of the medium alters the statistics of the photon trajectories, an effect that becomes more distinct as the source–detector spacing increases. In terms of photon propagation, the wavy layer boundary interfaces and the refractive index mismatch can be considered as an additional scattering process, the anisotropy of which is different to the scattering anisotropy of typical skin tissues. This could be important for the accurate determination of skin tissue optical properties when the source–detector spacing is small.

The results also suggest that all probe spacings up to 800 µm sample effectively the same vascular bed. If this is true, then the wider probe spacing is desirable, as a larger absorption signal from the blood is obtained. Also, each probe spacing should yield the same value for haemoglobin concentration and saturation. We are manufacturing a fibre-optic probe that will allow reflectance spectra to be gathered at all three spacings simultaneously. We can thus test this conclusion both in phantoms and in real skin.
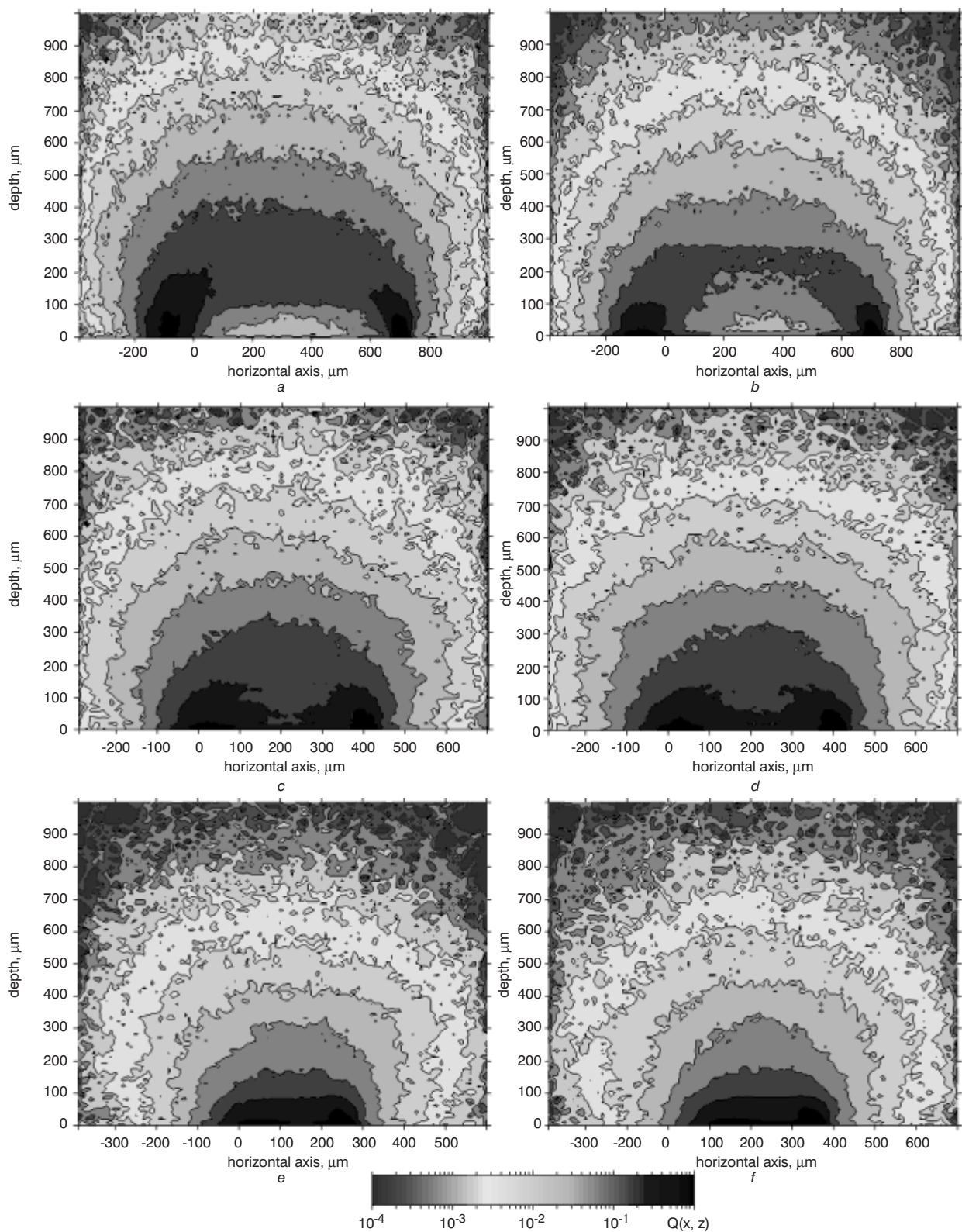
Fig. 4 *Two dimensional distributions of the spatial depth sensitivity for the wavy and flat interfaces between the layer boundaries of the skin model for the various source-detector fibre spacing. (a) and (b) 800 μm; (c) and (d) 400 μm; (e) and (f) 250 μm (centre to centre). Source and detector fibre diameters are 200 μm, and 50 μm, respectively, with numerical aperture 0.22. The assumed optical properties of the medium are given in Table 2*

5 Summary

In this paper, we have proposed a simple numerical method as a tool for the optimisation of probe geometry, so that the probe is preferentially sensitive to the optical properties at different depths within the skin. Figs 4 and 5 present the results of the simulation of the spatial localisation of the detected signal in multi-layered highly scattering complex medium with wavy and flat boundaries between the layers. Knowledge of this photon signal localisation is very important for the clinical interpretation of the results, as capillary loops are responsible for delivering nutrients to the epidermis, whereas deeper vessels are primarily thermoregulatory in function.

The results of the simulation show that, for the small source–detector separation (800 μm and smaller), rough boundaries between layers of different refractive indices can
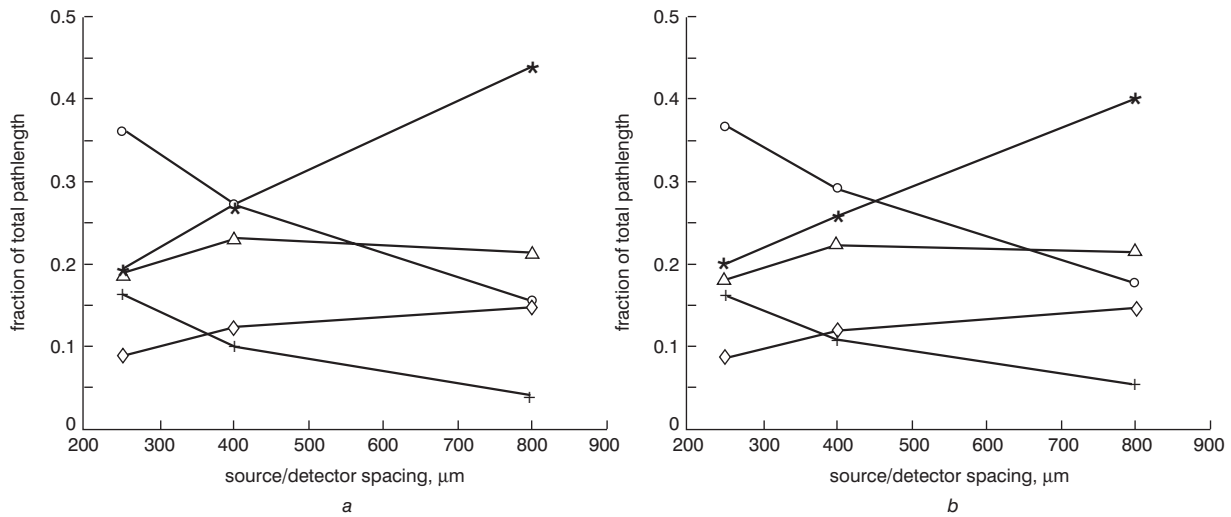
Fig. 5 *Fraction of total path length in the layers of modelling media: (a) for the medium with wavy layer boundary interfaces; (b) for the medium with flat layer boundary interfaces. Symbols '+', 'O', '△', '◇', and '✳' correspond to layers 1–5 respectively (see Table 2)*

play a significant role in skin optics. Wavy layer interfaces produce a deeper and more homogeneous distribution of photons within the skin and tend to suppress the direct channelling of photons from source to detector.

Our model predicts that a probe spacing of 250 μm samples primarily the epidermal layers and papillary dermis, whereas spacings of 400–800 μm sample the upper blood net dermis and dermis. In a subsequent paper, we will present experimental results obtained on real skin at all three probe spacings to validate this prediction.

References

ANDERSON, R. R., and PARRISH, J. A. (1982): 'Optical properties of human skin' in REGAN, J. D., and PARISH, J. A. (Eds): 'The science of photomedicine' (Pergamon Press, New York), pp. 147–194

ARRIDGE, S. (1995): 'Photon-measurement density functions. Part I: Analytical forms', *Appl. Opt.*, **34**, pp. 7395–7409

BORN, M., and WOLF, E. (1986): 'Principles of optics: electromagnetic theory of propagation, interference and diffraction of light, 6th edn' (Pergamon Press)

CASHWELL, E. D., and EVERETT, C. J. (1959): 'A practical manual on the Monte Carlo method for random walk problems' (Pergamon Press, London)

CHANCE, B. (1954): 'Spectrophotometry of intracellular respiratory pigments', *Science*, **120**, pp. 767–775

CHEONG, W. F., PRAHL, S. A., and WELCH, A. J. (1990): 'A review of the optical properties of biological tissues', *IEEE J. Quantum Electron.*, **26**, pp. 2166–2185

CORCUFF, P., BERTRAND, C., and LEVEQUE, J. L. (1993): 'Morphometry of human epidermis *in vivo* by real-time confocal microscopy', *Arch. Dermatol. Res.*, **285**, pp. 475–481

DE MUL, F. F., KOELINK, M. H., KOK, M. L., HARMSMA, P. J., GREVE, J., GRAAFF, R., and AARNOUDSE, J. G. (1995): 'Laser Doppler velocimetry and Monte Carlo simulation on models for blood perfusion in tissue', *Appl. Opt.*, **34**, pp. 6595–6611

DOORNBOS, R. M. P., LANG, R., AALDERS, M. C., CROSS, F. M., and STERENBORG, H. J. C. M. (1999): 'The determination of *in vivo* human tissue optical properties and absolute chromophore concentrations using spatially resolved steady-state diffuse reflectance spectroscopy', *Phys. Med. Biol.*, **44**, pp. 967–981

DUCK, F. A. (1990): 'Physical properties of tissue' (Academic Press, San Diego), pp. 43–71

FEATHER, J. W., DAWSON, J. B., BARKER, D. J., and COTTERILL, J. A. (1981): 'A theoretical and experimental study of optical properties of *in vivo* skin' in MARKS, R., and PAYNE, P. A. (Eds): 'Bioengineering and the skin' (MTP, Lancaster), pp. 275–281

HANNA, G. B., NEWTON, D. J., HARRISON, D. K., BELCH, J. J. F., and MCCOLLUM, P. T. (1995): 'Use of lightguide spectrophotometry to quantify skin oxygenation in variable model of venous hypertension', *Br. J. Surg.*, **82**, pp. 1352–1356

HIRAOKA, M., FIBRANK, M., ESSENPREIS, M., COPE, M., ARRIDGE, S. R., VAN DER ZEE, P., and DELPY, D. T. (1993): 'A Monte Carlo investigation of optical pathlength in homogeneous tissue and its application to near-infrared spectroscopy', *Phys. Med. Biol.*, **38**, pp. 1859–1876

HOLBROOK, K. A. (1991): 'Structure and functions of the developing human skin' in GOLDSMITH, L. A. (Ed.): 'Physiology, biochemistry, and molecular biology of the skin' (Oxford University Press, Oxford), **1**, pp. 63–112

JACQUES, S. L., and WANG, L. (1995): 'Monte Carlo modeling of light transport in tissues' in WELCH, A. J., and VAN GEMERT, M. J. C. (Eds): 'Optical-thermal response of laser-irradiated tissues' (Plenum Press, New York), pp. 73–100

JAKOBSSON, A., and NILSSON, G. E. (1993): 'Prediction of sampling depth and photon pathlength in laser Doppler flowmetry', *Med. Biol. Eng. Comput.*, **31**, pp. 301–307

KIENLE, A., LILGE, L., PATTERSON, M. S., HIBST, R., STEINER, R., and WILSON, B. C. (1996): 'Spatially resolved absolute diffuse reflectance measurements for noninvasive determination of the optical scattering and absorption coefficients of biological tissue', *Appl. Opt.*, **35**, pp. 2304–2314

MAIBACH, H. T., and LOWE, N. L. (1987): 'Models in dermatology' (Karger, New York)

MEIER, R. R., LEE, J.-S., and ANDERSON, D. E. (1978): 'Atmospheric scattering of middle uv radiation from an internal source', *Appl. Opt.*, **17**, pp. 3216–3225

NILSSON, H., and NILSSON, G. E. (1998). 'Monte Carlo simulations of the light interaction with blood vessels in human skin in the red wavelength region', *Proc. SPIE*, **3252**, pp. 44–53

ODLAND, G. F. (1991): 'Structure of the skin' in GOLDSMITH, L. A. (Ed.): 'Physiology, biochemistry, and molecular biology of the skin' (Oxford University Press, Oxford), **1**, pp. 3–62

OKADA, E., FIRBANK, M., SCHWEIGER, M., ARRIDGE, S. R., COPE, M., and DELPY, D. T. (1997): 'Theoretical and experimental investigation of near-infrared light propagation in a model of the adult head', *Appl. Opt.*, **36**, pp. 21–31

PRAHL, S. A., KEIJZER, M., JACQUES, S. L., and WELCH, A. J. (1989): 'A Monte Carlo model of light propagation in tissue', *SPIE Inst. Series*, **IS5**, pp. 102–111

RAJADHYAKSHA, M., and ZAVISLAN, J. M. (1998): 'Confocal reflectance microscopy of unstained tissue *in vivo*', *Clin. Exp. Techniques*, **14**, pp. 26–30

RYAN, T. J. (1991): 'Cutaneous circulation' in GOLDSMITH, L. A. (Ed.): 'Physiology, biochemistry, and molecular biology of the skin' (Oxford University Press, Oxford), **2**, pp. 1019–1084

SCHMITT, J. M., and KUMAR, G. (1998): 'Optical scattering properties of soft tissue: a discrete particle model', *Appl. Opt.*, **37**, pp. 2788–2797

SERUP, J., and JEMEC, G. B. E. (Eds) (1995): 'Skin surface contour evaluation' in 'Non-invasive methods and the skin' (CRC Press, Inc., Boca Raton), chap. 5, pp. 83–131

SHEUPLEIN, R. J. (1964): 'A survey of some fundamental aspects of the absorption and reflection of light by tissues', *J. Soc. Cosmet. Chem.*, **15**, pp. 155–156

SIMPSON, C. R., KOHL, M., ESSENPREIS, M., and COPE, M. (1998): 'Near-infrared optical properties of *ex vivo* human skin and subcutaneous tissues measured using the Monte Carlo inversion technique', *Phys. Med. Biol.*, **43**, pp. 2465–2478

SLINEY, D., and WOLBARSHT, M. (1980): 'Optical radiation hazards to the skin' in 'Safety with lasers and others optical sources. A comprehensive handbook' (Plenum Press, New York), pp. 161–185

STENN, K. S. (1988): 'The skin' in WEISS, L. (Ed.): 'Cell and tissue biology' (Urban & Shwarzenberg, Baltimore), pp. 541–572

TUCHIN, V. V., UTZ, S. R., and YAROSLAVSKY, I. V. (1994): 'Tissue optics, light distribution, and spectroscopy', *Opt. Eng.*, **33**, pp. 3178–3188

TUCHIN, V. V. (1998): 'Lasers and fiber optics in biomedical investigations (in Russian)' (Saratov State University Press, Saratov)

VAN DER ZEE, P. (1992): 'Measurement and modeling of the optical properties of human tissue in the near infrared'. PhD dissertation, University of London, p. 313

WANG, L., JACQUES, S. L., and ZHENG, L. (1995): 'MCML—Monte Carlo modeling of light transport in multi-layered tissues', *Comput. Methods Programs Biomed.*, **47**, pp. 131–146

YOO, K. M., LIU, F., and ALFANO, R. R. (1990): 'When does the diffusion approximation fail to describe photon transport in random media?', *Phys. Rev. Lett.*, **64**, pp. 2647–2650

YOUNG, A. R. (1997): 'Chromophores in human skin', *Phys. Med. Biol.*, **42**, pp. 789–802

Author's biography

IGOR V. MEGLINSKY was born in Saratov, Russia, in 1968. He received his BSc and MSc in Laser Physics from the Department of Physics, Saratov State University, Russia. After pre-doctoral research at the Department of Biochemistry and Biophysics, University of Pennsylvania, USA, he obtained his PhD in Biophysics in 1997 from Saratov State University. Since 1998, he has been a research fellow at the School of Physics, University of Exeter, Exeter. He is currently lecturing at the School of Mechanical Engineering, University of Cranfield, Bedfordshire.